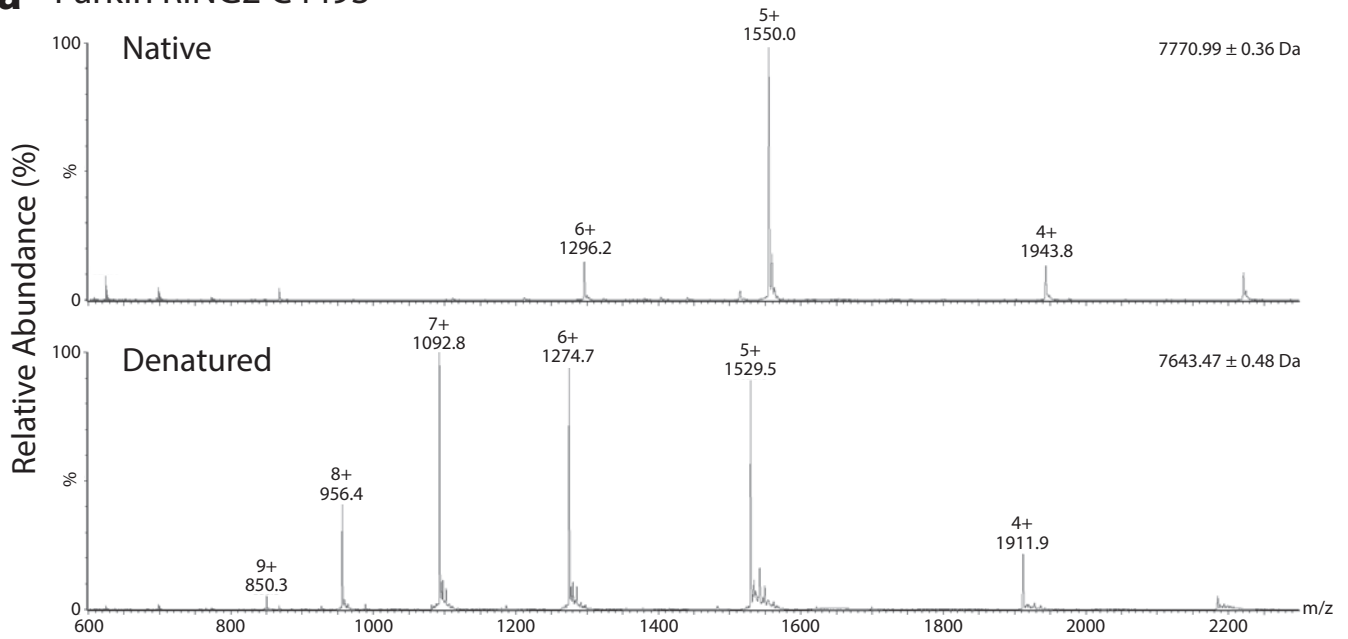


Supplementary Figure S1. Analytical ultracentrifugation analysis of parkin RING2 C449S.

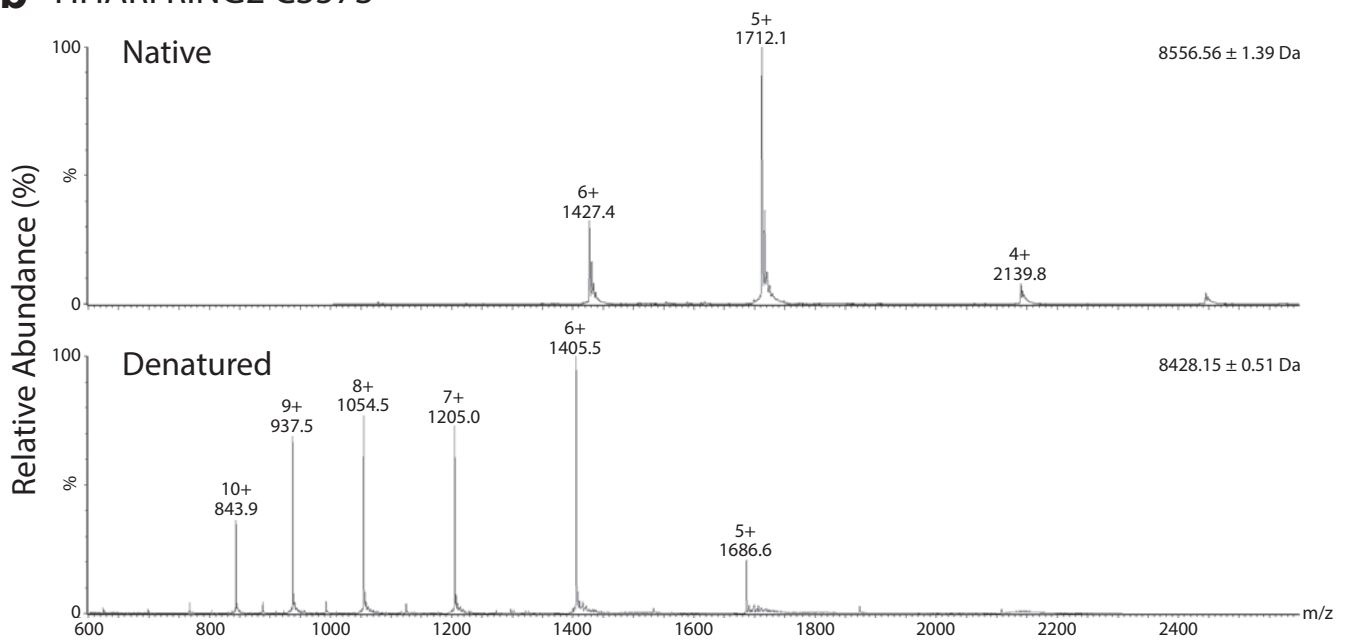
(a) Overlay scans from sedimentation velocity experiments at 25 °C at a rotor speed of 60,000 rpm with scans collected at 10 min intervals. The data was fit to a singular species ($s_{20,w}$ of 1.20 S).

(b) Representative sedimentation equilibrium experiment collected at 25 °C at 43,000 rpm. Data were fit to an ideal single species model and gave a calculated mass of 7.73 ± 0.06 kDa (MM_{calc} with 2 Zn^{2+} ions = 7.77 kDa; $R^2 = 0.99$). The residuals from the fitting are shown as an inset.

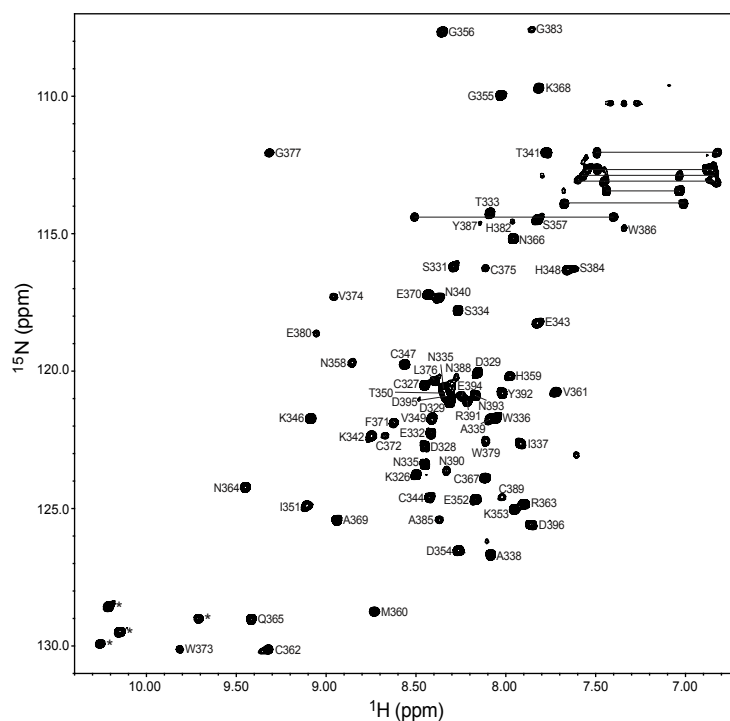
a Parkin RING2 C449S



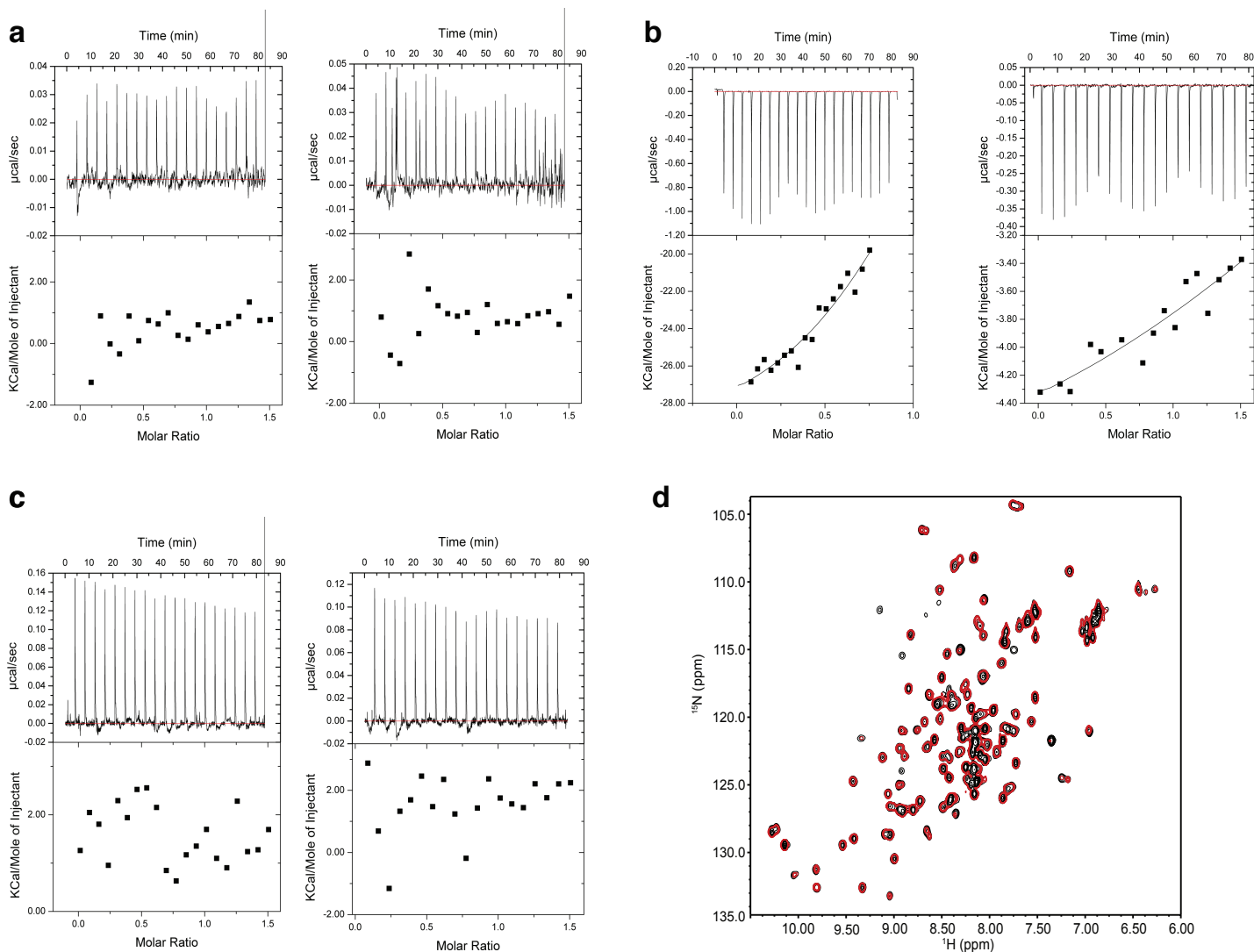
b HHARI RING2 C357S



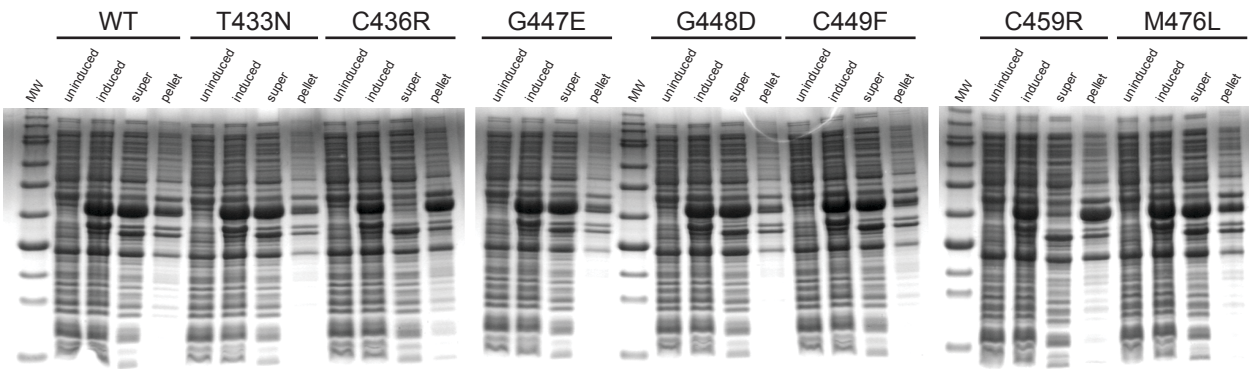
Supplementary Figure S2. Raw ESI-MS spectra for native and denatured (A) parkin RING2 C449S and (B) HHARI RING2 C357S.



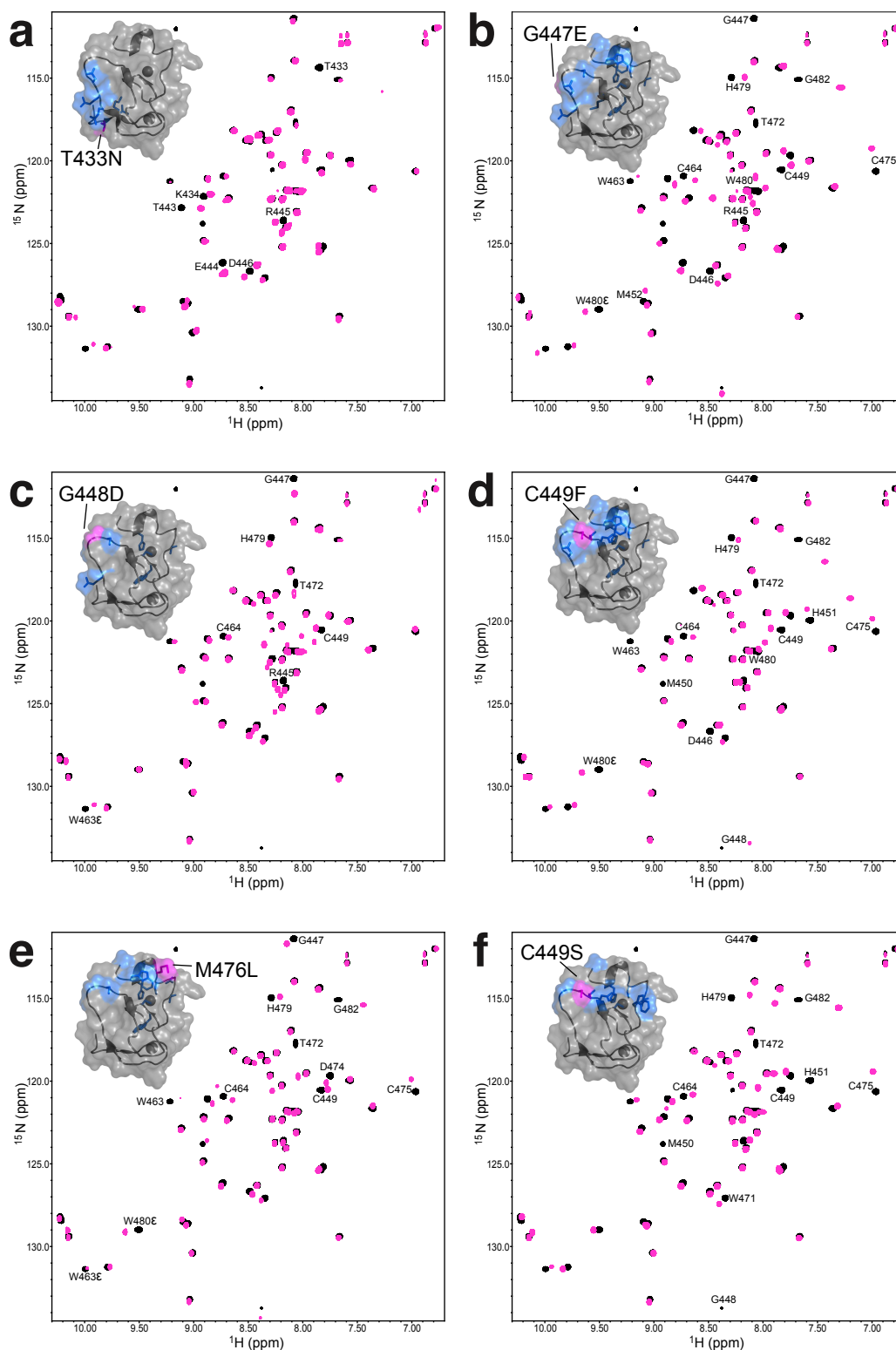
Supplementary Figure S3. Assigned 600 MHz ^1H - ^{15}N HSQC spectrum of $^{13}\text{C}^{15}\text{N}$ -labeled HHARI RING2 C357S (300 μM in 20 mM Tris-HCl, 120 mM NaCl, 5 mM DTT, pH 6.5) showing that the protein is well folded. The spectrum is labeled using the one-letter amino acid code and residue number according to the human HHARI sequence. Tryptophan N ϵ 1 amides are indicated (*).



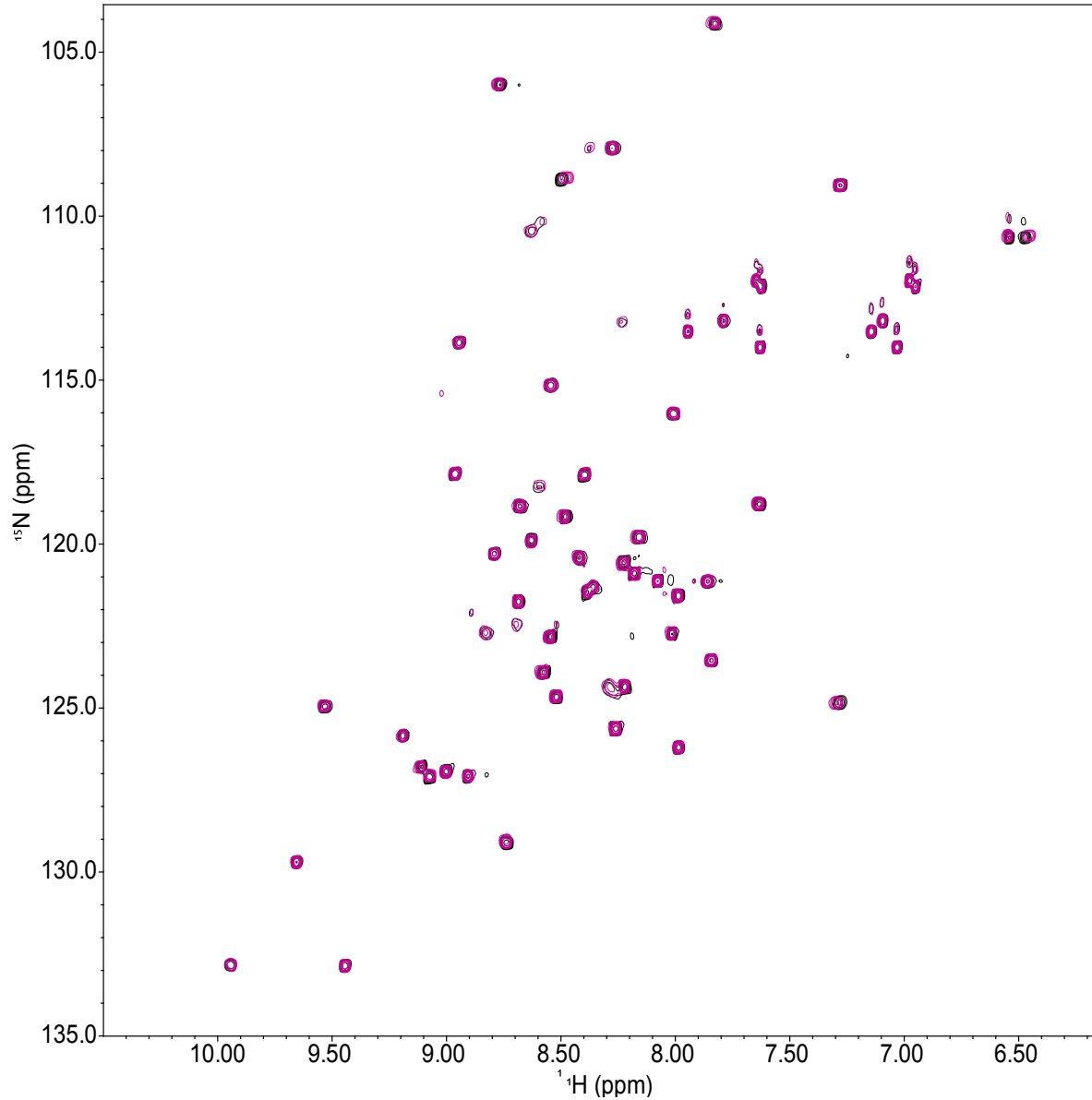
Supplementary Figure S4. Isothermal calorimetry and NMR spectroscopy shows that parkin IBR and RING2 domains are not E2 recruiting domains. ITC curves showing the lack of interaction of parkin (a) IBR, (b) RING2 and (c) IBR-RING2 domains with Ubch7 and Ubch8 E2 proteins. Each panel shows a titration experiment completed at 18°C for Ubch7 (left) and Ubch8 (right). In panel (d) the NMR spectrum of ^{15}N -labeled IBR-RING2 is shown alone (black contours) and with the addition of two equivalents of Ubch7 (red contours). Spectra were acquired in 20 mM Tris-HCl, 120 mM NaCl, 1 mM DTT, pH 7.5 at 25°C.



Supplementary Figure S5. Expression and solubility tests for GST-fusion wild-type parkin RING2 and ARJP substitutions assessed by SDS-PAGE.

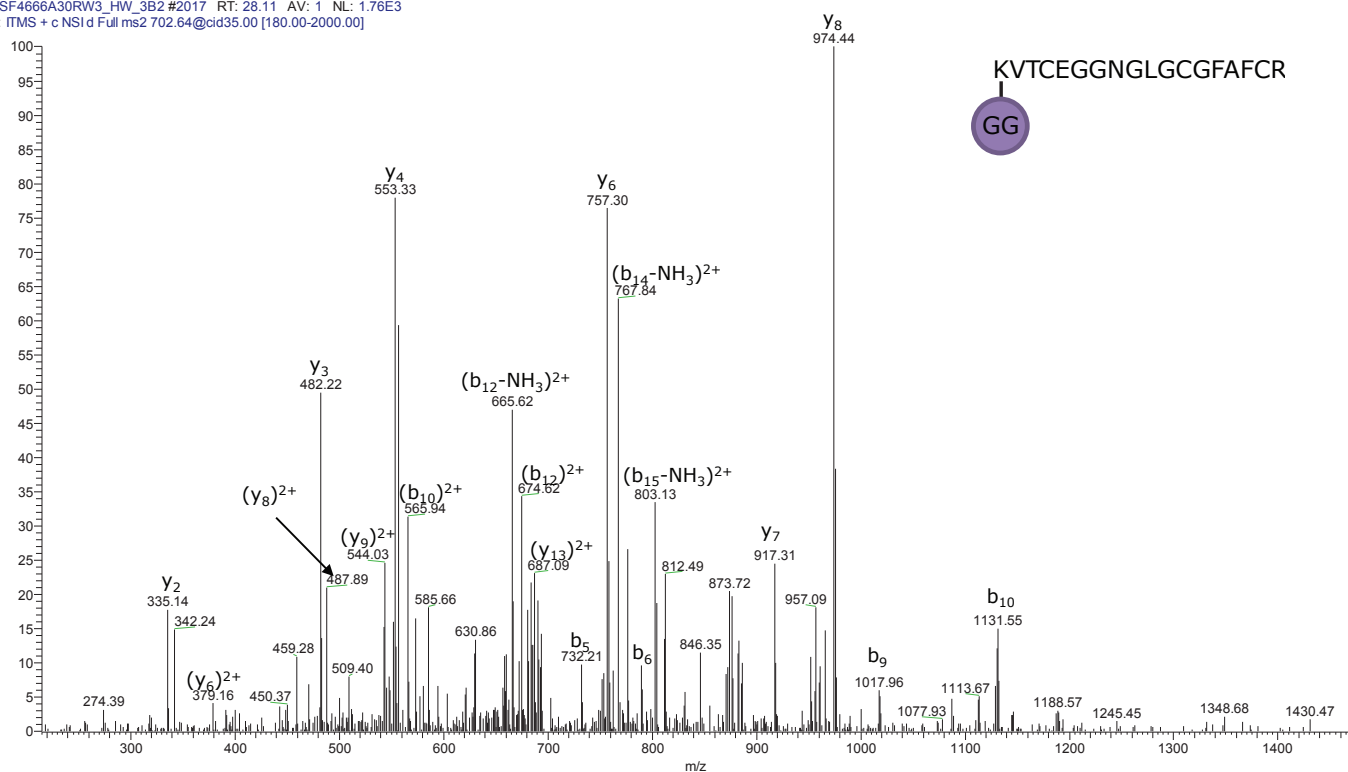


Supplementary Figure S6. ^1H - ^{15}N HSQC spectra of parkin RING2 and ARJP substitutions. Spectral overlays for wild-type parkin RING2 with ARJP substituted protein (magenta) for (a) T433N, (b) G447E, (c) G448D, (d) C449F, (e) M476L, and (f) C449S. Amides that demonstrated the largest chemical shift perturbation are labeled and mapped on to the parkin RING2 structure (insets).



Supplementary Figure S7. Titration of unlabeled fly parkin RING2⁴¹⁷⁻⁴⁸² into ¹⁵N-labeled fly parkin IBR³⁴²⁻⁴⁰². The data shows the 600 MHz ¹H-¹⁵N HSQC spectrum of ¹⁵N-labelled IBR (black contours) and upon the addition of two equivalents of RING2 (magenta). Spectra were acquired in 25 mM Tris-HCl, 150 mM NaCl, 1 mM DTT, pH 7.5 at 25°C.

PSF466A30RW3_HW_3B2 #2017 RT: 28.11 AV: 1 NL: 1.76E3
T: ITMS + c NSI d Full ms2 702.64@cid35.00 [180.00-2000.00]



Supplementary Figure S8. MS-MS data showing the identity of a ubiquitinated site at position K349 of human parkin. The site of ubiquitination was confirmed following trypsin digest of Δ Ubl parkin following an ubiquitination reaction. Peaks in the spectrum denoting y and b ions are labeled for the sequence K349-R366 (shown above). The $(y_8)^{2+}$ confirms the identity of the GG isopeptide linkage on the sequence.

Figure 3c

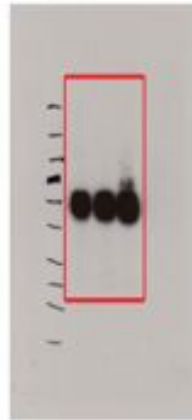


α -Parkin



α -His

Figure 3f

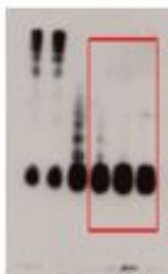


α -Parkin

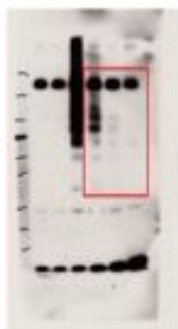


α -His

Figure 3g

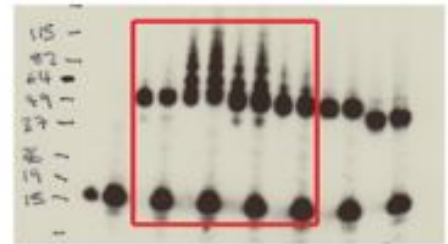
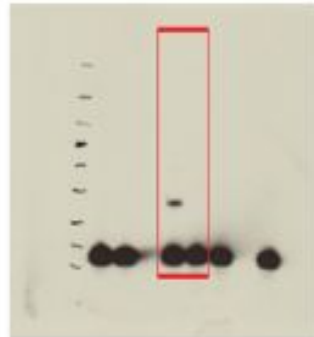


α -Parkin



α -His

Figure 6a



Supplementary Figure S9. Original Western blot data for autoubiquitination assays for parkin. Red boxes denote the regions of the original data presented in the corresponding figures.

Supplementary Table S1. Structural Statistics for 20 lowest energy structures of parkin RING2

NMR distance and dihedral constraints

Distance constraints	
Total NOE	575
Intra-residue	165
Inter-residue	
Sequential ($ i-j = 1$)	151
Medium-range ($ i-j < 4$)	72
Long-range ($ i-j > 5$)	187
Intermolecular	
Hydrogen bonds	0
Zinc restraints	24
Total dihedral angle restraints ¹	
phi	11
psi	11

Structure statistics

Violations (mean and s.d.)	
Distance constraints (Å)	0.042 ± 0.003
Dihedral angle constraints (°)	0.340 ± 0.259
Max. dihedral angle violation (°)	4.2
Max. distance constraint violation (Å) ²	0.57
Deviations from idealized geometry ³	
Bond lengths (Å)	0.006 ± 0.000
Bond angles (°)	0.606 ± 0.027
Improper (°)	0.814 ± 0.062
Average pairwise r.m.s.d. (Å) ⁴	
Heavy	1.231 ± 0.197
Backbone	0.818 ± 0.173

¹Psi/Psi dihedral restraints determined using TALOS+

²One NOE violation > 0.5 Å over all 20 models

³As reported by Xplor-NIH

⁴Pairwise r.m.s.d. was calculated among 20 refined structures (residues T433-E444, H451-C464, C475-H479)

Supplementary Table S2. Cysteines involved in Zn²⁺-coordination in parkin RING2 and HHARI RING2 domains determined using C α and C β chemical shifts.

Parkin RING2 (residues 417-482)

Cys Chemical Shifts (ppm) ^a								
	<u>C436 (I)^b</u>	<u>C439 (I)</u>	<u>C449 (cat)</u>	<u>C454 (I)</u>	<u>C459 (I)</u>	<u>C464 (II)</u>	<u>C467 (II)</u>	<u>C475 (II)</u>
C α	56.940	59.333	59.260	61.623	60.490	58.091	57.134	64.610
C β	31.690	31.555	28.133	31.826	30.002	32.693	31.658	29.092
Probabilities^c								
Oxidized	0.0%	0.0%	0.0%	0.0%	0.0%	0.0%	0.0%	0.0%
Reduced	13.9%	2.5%	99.2%	0.4%	9.8%	5.5%	12.4%	4.6%
Zn ²⁺ -coordinated	86.1%	97.5%	0.8%	99.6%	90.2%	94.5%	87.6%	95.4%

HHARI RING2 (residues 325-396)

Cys Chemical Shifts (ppm) ^a									
	<u>C327 (N)</u>	<u>C344 (I)</u>	<u>C347 (I)</u>	<u>C357 (cat)</u>	<u>C362 (I)</u>	<u>C367 (I)</u>	<u>C372 (II)</u>	<u>C375 (II)</u>	<u>C389 (II)</u>
C α	58.528	56.386	59.186	ND ^d	61.820	60.891	56.771	58.459	60.418
C β	28.230	31.739	31.533	ND	31.457	32.564	33.703	32.140	29.791
Probabilities^c									
Oxidized	0.0%	0.0%	0.0%	ND	0.0%	0.0%	0.0%	0.0%	0.0%
Reduced	99.3%	19.7%	2.9%	ND	0.4%	0.6%	29.4%	3.9%	16.0%
Zn ²⁺ -coordinated	0.7%	80.3%	97.1%	ND	99.6%	99.4%	70.6%	96.1%	84.0%

^a determined using 3D CBCA(CO)NH and HNCACB experiments

^b identifiers to describe where the Cys residue is located in the RING2 protein – (I) involved in Zn²⁺-coordination Site I; (II) - involved in Zn²⁺-coordination Site II; (cat) - conserved catalytic cysteine; (N) – located in the unstructured N-terminus

^c probability calculation based upon Kornhaber *et al.*, 2006. The most probable condition for each cysteine is highlighted in bold

^d C α and C β chemical shifts for HHARI C357 not determined, data collected on HHARI RING2 C357S

Supplementary Table S3. Structural Statistics for 20 lowest energy structures of parkin IBR-RING2

NMR distance and dihedral constraints

Distance constraints ¹	
Total NOE	611 / 447 / 1156
Intra-residue	156 / 143 / 360
Inter-residue	
Sequential ($ i - j = 1$)	201 / 117 / 353
Medium-range ($ i - j < 4$)	65 / 48 / 115
Long-range ($ i - j > 5$)	189 / 139 / 328
Intermolecular	- / - / 0
Hydrogen bonds	0 / 0 / 0
Zinc restraints	24 / 24 / 48
Total dihedral angle restraints ²	
phi	22 / 25 / 47
psi	22 / 25 / 47

Structure statistics

Violations (mean and s.d.)	
Distance constraints (Å)	0.040 ± 0.002
Dihedral angle constraints (°)	0.467 ± 0.080
Max. dihedral angle violation (°)	7.5
Max. distance constraint violation (Å) ³	0.7
Deviations from idealized geometry ⁴	
Bond lengths (Å)	0.006 ± 0.000
Bond angles (°)	0.550 ± 0.022
Impropers (°)	0.758 ± 0.056
Average pairwise r.m.s.d. (Å) ⁵	
Heavy	2.268 ± 0.304 / 2.316 ± 0.306
Backbone	1.208 ± 0.258 / 1.393 ± 0.245

¹ For IBR (E342-L396) / RING2 (K430-G482) / IBR-RING2 (E342-G482)

² Psi/Psi dihedral restraints determined using TALOS+

³ Total of 4 NOE violations > 0.5 Å over all 20 models

⁴ As reported by Xplor-NIH

⁵ Pairwise r.m.s.d. was calculated among 20 refined structures (IBR, residues V351-I392; RING2, residues K430-W480)

Supplementary Table S4. Cysteines involved in Zn²⁺-coordination in *Drosophila* and human parkin IBR-RING2 domains determined using C α and C β chemical shifts.

***Drosophila* Parkin IBR-RING2 (residues 342-482)**

		Cys Chemical Shifts (ppm) ^a																
		C353 (I) ^b	C358 (I)	C368 (NC)	C373 (I)	C377 (I)	C382 (II)	C385 (II)	C394 (II)	C407 (NC)	C436 (I)	C439 (I)	C449 (cat)	C454 (I)	C459 (I)	C464 (II)	C467 (II)	C475 (II)
C α		57.731	60.268	58.581	58.504	59.988	57.691	58.112	59.835	58.713	57.016	59.348	59.291	61.571	60.499	57.776	56.999	64.533
C β		31.865	29.375	28.450	28.311	32.365	32.475	32.359	30.761	28.102	31.698	31.196	28.000	32.045	30.174	32.930	31.870	29.092
Probabilities^c																		
Oxidized		0.0%	0.0%	0.0%	0.0%	0.0%	0.0%	0.0%	0.0%	0.0%	0.0%	0.0%	0.0%	0.0%	0.0%	0.0%	0.0%	0.0%
Reduced		7.3%	39.8%	98.3%	99.1%	1.2%	7.0%	5.0%	4.1%	99.5%	13.2%	3.5%	99.5%	0.3%	6.8%	7.8%	12.3%	4.9%
Zn ²⁺ coordinated		92.7%	60.2%	1.7%	0.9%	98.8%	93.0%	95.0%	95.9%	0.5%	86.8%	96.5%	0.5%	99.7%	93.2%	92.2%	87.7%	95.1%

Human Parkin IBR-RING2 (residues 321-465)

		Cys Chemical Shifts (ppm) ^a																
		C323 (N)	C332 (I)	C337 (I)	C352 (I)	C360 (I)	C365 (II)	C368 (II)	C377 (II)	C418 (I)	C421 (I)	C431 (cat)	C436 (I)	C441 (I)	C446 (II)	C449 (II)	C451 (NC)	C457 (II)
C α		ND ^d	57.694	60.528	59.851	59.537	58.119	58.828	60.387	56.136	59.678	59.111	60.914	62.229	58.147	ND	ND	ND
C β		ND	32.329	29.637	29.495	32.329	31.904	32.187	30.770	32.754	31.904	28.361	32.187	32.754	32.471	ND	ND	ND
Probabilities^c																		
Oxidized		ND	0.0%	0.0%	0.0%	0.0%	0.0%	0.0%	0.0%	0.0%	0.0%	0.0%	0.0%	0.0%	0.0%	ND	ND	ND
Reduced		ND	68.7%	20.6%	39.6%	1.7%	5.4%	2.9%	2.6%	22.2%	1.6%	98.2%	0.6%	0.2%	5.0%	ND	ND	ND
Zn ²⁺ coordinated		ND	93.1%	79.4%	60.4%	98.3%	94.6%	97.1%	97.4%	77.8%	98.4%	1.8%	99.4%	99.8%	95.0%	ND	ND	ND

^a determined using 3D CBCA(CO)NH and HNCACB experiments

^b identifiers to describe where the Cys residue is located in the IBR or RING2 protein – (I) involved in Zn²⁺-coordination Site I; (II) - involved in Zn²⁺-coordination Site II; (cat) - conserved catalytic cysteine; (N) – located in the unstructured N-terminus; (NC) - non Zn²⁺ coordinating residue

^c probability calculation based upon Kornhaber *et al.*, 2006. The most probable condition for each cysteine is in bold.

^d C α and C β chemical shifts not determined